JACS
JOURNAL OF THE AMERICAN CHEMICAL SOCIETY
Article
pubs.acs.org/JACS

Peroxo and Superoxo Moieties Bound to Copper Ion: Electron-Transfer Equilibrium with a Small Reorganization Energy

Rui Cao,[†] Claudio Saracini,[†,#] Jake W. Ginsbach,[‡,∥] Matthew T. Kieber-Emmons,[‡,⊥] Maxime A. Siegler,[†] Edward I. Solomon,[*,‡] Shunichi Fukuzumi,[*,§,#] and Kenneth D. Karlin[*,†]

[†]Department of Chemistry, Johns Hopkins University, Baltimore, Maryland 21218, United States

[‡]Department of Chemistry, Stanford University, Stanford, California 94305, United States

[§]Faculty of Science and Engineering, ALCA, SENTAN, Japan Science and Technology Agency (JST), Meijo University, Nagoya, Aichi 468-0073, Japan

[#]Department of Chemistry and Nano Science, Ewha Womans University, Seoul 120-750, Korea

Supporting Information

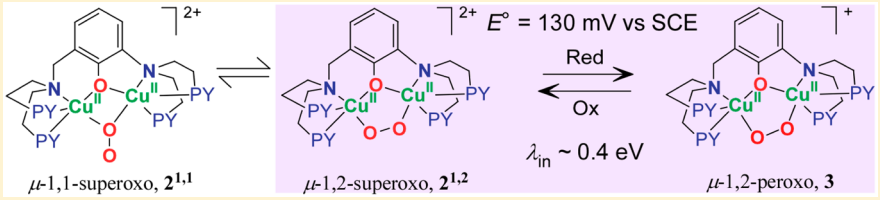

ABSTRACT: Oxygenation of $[Cu_2(UN\text{-}O^-)(DMF)]^{2+}$ (**1**), a structurally characterized dicopper Robin–Day class I mixed-valent Cu(II)Cu(I) complex, with UN-O$^-$ as a binucleating ligand and where dimethylformamide (DMF) binds to the Cu(II) ion, leads to a superoxo-dicopper(II) species $[Cu^{II}_2(UN\text{-}O^-)(O_2^{\bullet-})]^{2+}$ (**2**). The formation kinetics provide that $k_{on} = 9 \times 10^{-2}$ M^{-1} s^{-1} (−80 °C), $\Delta H^{\ddagger} = 31.1$ kJ mol^{-1} and $\Delta S^{\ddagger} = -99.4$ J K^{-1} mol^{-1} (from −60 to −90 °C data). Complex **2** can be reversibly reduced to the peroxide species $[Cu^{II}_2(UN\text{-}O^-)(O_2^{2-})]^{+}$ (**3**), using varying outer-sphere ferrocene or ferrocenium redox reagents. A Nernstian analysis could be performed by utilizing a monodiphenylamine substituted ferrocenium salt to oxidize **3**, leading to an equilibrium mixture with $K_{et} = 5.3$ (−80 °C); a standard reduction potential for the superoxo–peroxo pair is calculated to be $E^{\circ} = +130$ mV vs SCE. A literature survey shows that this value falls into the range of biologically relevant redox reagents, e.g., cytochrome *c* and an organic solvent solubilized ascorbate anion. Using mixed-isotope resonance Raman (rRaman) spectroscopic characterization, accompanied by DFT calculations, it is shown that the superoxo complex consists of a mixture of μ-1,2- (**2**^{1,2}) and μ-1,1- (**2**^{1,1}) isomers, which are in rapid equilibrium. The electron transfer process involves only the μ-1,2-superoxo complex $[Cu^{II}_2(UN\text{-}O^-)(\mu\text{-}1,2\text{-}O_2^{\bullet-})]^{2+}$ (**2**^{1,2}) and μ-1,2-peroxo structures $[Cu^{II}_2(UN\text{-}O^-)(O_2^{2-})]^{+}$ (**3**) having a small bond reorganization energy of 0.4 eV (λ_{in}). A stopped-flow kinetic study results reveal an outer-sphere electron transfer process with a total reorganization energy (λ) of 1.1 eV between **2**^{1,2} and **3** calculated in the context of Marcus theory.

INTRODUCTION

Molecular oxygen (dioxygen; O_2) is abundant and an important energy source via its combustion of fuels (e.g., hydrocarbons, H_2, etc.) most often leading to water as byproduct. Dioxygen is also nature's primary source for energy production via cellular respiration. In cytochrome *c* oxidase, the terminal respiratory oxidase, a heme-copper active site mediates four-electron-four-proton reduction of O_2 to water eq 1 to generate a proton motive force for downstream ATP synthesis.[1] In the "reverse" process, plants and algae harness sunlight through photosynthesis to replenish the earth with dioxygen, converting and storing 130 terawatt equiv of energy per year eq 2.[2] Less is understood concerning this water oxidation chemistry where manganese cluster bound water molecules facilitate oxidative coupling and O–O bond formation to give dioxygen, possibly via an as yet undetected peroxide or superoxide Mn-species intermediates.[3]

$$O_2 + 4H^+ + 4e^- \xrightarrow{\text{respiration}} 2H_2O \quad (1)$$

$$O_2 + 4H^+ + 4e^- \xleftarrow{\text{photosynthesis, } h\nu} 2H_2O \quad (2)$$

In biology, Fe/Cu or Cu and Mn protein active-site complexes mediate dioxygen reduction and water oxidation, respectively. It is useful to consider either process in the context of O_2 reduction in metal-free aqueous solution (Figure 1a). There, the nature of the (ir)reversible steps are understood and reduction potentials and pK_a's are known, see Figure 1a.[4] However, such thermodynamic data are generally lacking when it comes to O_2 and reduced derivatives when they are bound to metal ions, especially copper. At a fundamental level of knowledge, to uncover how biological transformations occur, such as dioxygen (or derivatives) utilizing reactions in hemes, nonheme iron, copper and manganese enzymes, and/or to build practical and efficient systems for carrying out such reactions as O_2 reduction

Received: March 5, 2016
Published: May 26, 2016

DOI: 10.1021/jacs.6b02404
J. Am. Chem. Soc. 2016, 138, 7055–7066

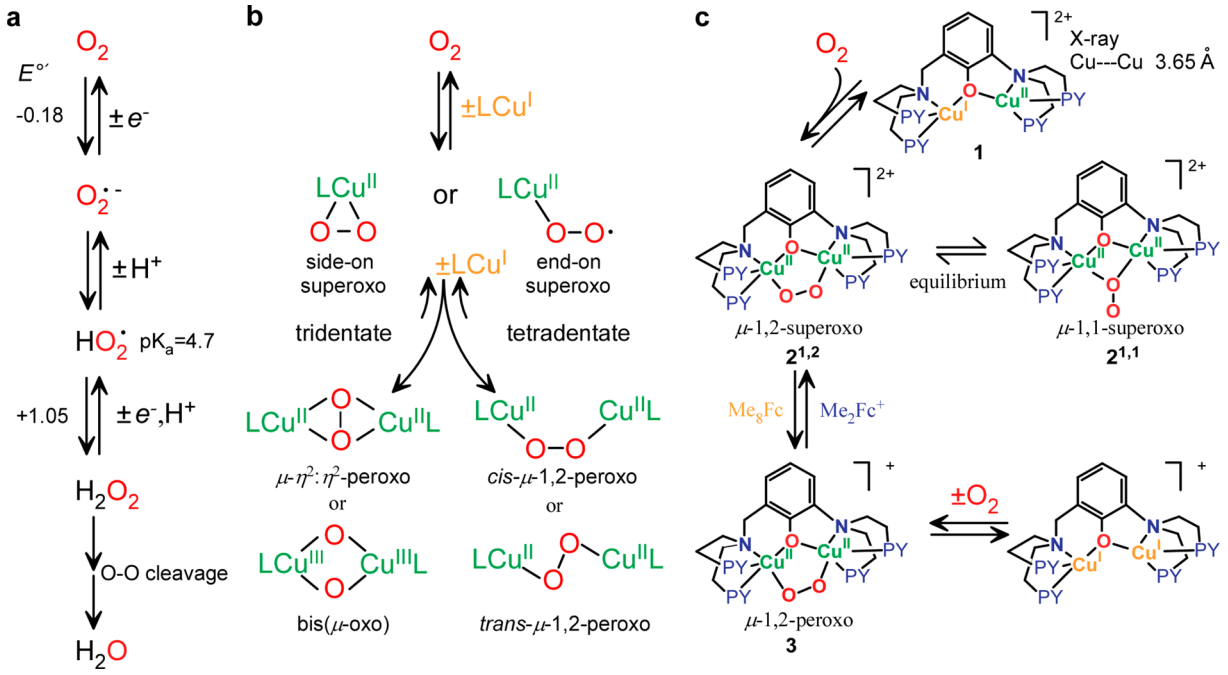

Figure 1. Oxygen reduction and modeling chemistry. (a) Reduction of molecular oxygen in aqueous media. $E^{\circ\prime}$ values are the reduction potentials at pH 7 versus NHE[4] {Note: In the text, reduction potential values have been converted to versus SCE, as follows: E_{SCE} (V) = E_{NHE} (V) − 0.242 (V)}. (b) Model chemistry of mononuclear LCu^{I} and dinuclear LCu^{I}—$Cu^{I}L$ centers and their reversible reactions with dioxygen. (c) The phenolate-bridged mixed-valent Cu^{I}—Cu^{II} complex $[Cu^{I}Cu^{II}(UN\text{-}O^{-})]^{2+}$ (**1**) (UN-OH = 2-(bis(2-(pyridin-2-yl)ethyl)amino)-6-((bis(2-(pyridin-2-yl)ethyl)amino)-methyl)phenol, UN-O^{-} is the corresponding phenolate) reacts with dioxygen to form a superoxide species, either $\mathbf{2}^{1,1}$ or $\mathbf{2}^{1,2}$, which are in rapid equilibrium (see text). As previously reported, oxygenation of the phenolate dicopper(I) complex $[Cu^{I}_{2}(UN\text{-}O^{-})]^{+}$ gives the peroxide species $[Cu^{II}_{2}(UN\text{-}O^{-})(O_2^{2-})]^{+}$ (**3**). At the center of attention in this report is the interconversion chemistry of $\mathbf{2}^{1,2}$ and **3** via the use of outer-sphere ferrocenium derived redox agents.

to water or hydrogen peroxide (i.e., for fuel cells) or water oxidation catalysis, those reactions which are critical to societal energy concerns, the interrelationships of superoxide, (hydro)-peroxide and hydroxyl radical must be elucidated wherein entities are bound to metal ions in various environments.

For example, what are the reaction mechanisms for metal-superoxide conversion to metal-peroxide or hydroperoxide species, these in principle being reversible processes involving species with intact O—O bonds? What are the relevant thermodynamics? Surprisingly, even the conversion of a heme-superoxide ("oxy" heme) to heme-(hydro)peroxide (i.e., electron/proton addition), as occurs in the very well studied enzyme P450 monooxygenase enzymes, or their synthetic model compounds, is not thoroughly studied in terms of reaction mechanism or elucidation of applicable thermodynamic parameters.[5]

For an O_2-derived species bound to one or several metal ions, thermodynamic properties relating to redox or protonation will be considerably altered, whether or not in water, in organic solvent, or in a protein active site. For the latter, great variability in local dielectric environment and presence of second-sphere effects (e.g., local amino acid-derived dipoles, or H-bonding groups) may occur, potentially changing the inherent thermodynamic properties. The complexity of the metal—oxygen species' chemistry is increased by the possibility of having varying superoxide or peroxide coordination modes which likely depends on the nature of the metal ion's surrounding environment, that defined by a ligand or first coordination sphere at an enzyme active site. Depending on ligand denticity (e.g., tridentate or tetradentate), a superoxide moiety ligated to copper(II) ion may be bound in an side-on (η^2) or end-on fashion (Figure 1b).[6]

Another type of complexity occurs if there are two (or more) metal ions bound to the (su)peroxo entity. Dinuclear Cu_2O_2 species commonly form in LCu^{I}—O_2 chemistry, deriving from the reversible reaction of a cupric superoxide complex with a second mole equiv of the original LCu^{I} chelate. Most generally, if the ligand (L) is a tridentate donor, either a η^2:η^2-peroxo or bis-μ-oxo product forms (Figure 1b). By contrast, with tetradentate ligands, cupric-superoxide species are led to form *trans*-μ-1,2-peroxo- or *cis*-μ-1,2-peroxo-dicopper(II) complexes (Figure 1b).[6,7]

For the system we describe here, a phenol-containing binucleating ligand (UN-O^{-}) is employed, giving rise to a series of phenolate-bridged dicopper complexes of various types. We previously showed that a mixed-valent phenolate-bridged Cu(I)Cu(II) complex, $[Cu^{I}Cu^{II}(UN\text{-}O^{-})]^{2+}$ (**1**), reacts with molecular oxygen in a reversible manner, under cryogenic conditions, to give a superoxide-dicopper(II) complex, $[Cu^{II}_{2}(UN\text{-}O^{-})(O_2^{\bullet-})]^{2+}$ (**2**) (Figure 1c).[8] A closely related species, a peroxo analogue $[Cu^{II}_{2}(UN\text{-}O^{-})(O_2^{2-})]^{+}$ (**3**), was generated when the dicopper(I) precursor complex $[Cu^{I}_{2}(UN\text{-}O^{-})]^{+}$ is (reversibly) oxygenated (Figure 1c).[9]

To carry out this study with biologically relevant copper ion, ligand design and adaption of low-temperature manipulations and characterization techniques have had to be applied. In this report, motivated by the need for determining fundamentally important properties of metal-bound oxygen-derived species, we provide a rare case where an equilibrium constant and therefore reduction potential, plus a reorganization energy (Marcus theory lambda (λ) value) can be determined for the outer-sphere electron transfer interconversion of a superoxo and peroxo moiety bound to a dicopper center. The species involved are the

DOI: 10.1021/jacs.6b02404
J. Am. Chem. Soc. 2016, 138, 7055−7066

metal bound μ-1,2-superoxide moiety in $\mathbf{2}^{1,2}$ and the μ-1,2-peroxide ligand in complex **3** (Figure 1c). Resonance Raman spectroscopic and DFT analysis also reveals that $\mathbf{2}^{1,2}$ is in fast equilibrium with a structural isomer, the μ-1,1-superoxide complex $\mathbf{2}^{1,1}$ (Figure 1c).

RESULTS AND DISCUSSION

Synthesis and Crystal Structure of Mixed-Valent Complex $[Cu^{I}Cu^{II}(UN\text{-}O^{-})(DMF)]^{2+}$ (1). After improving on previously developed procedures, the complex **1** could be isolated as single crystal with one coordinated dimethylformamide (DMF) molecule, following the one-electron oxidation of the dicopper(I) complex $[Cu^{I}_{2}(UN\text{-}O^{-})]^{+}$ with ferrocenium hexafluoroantimonate ($FcSbF_6$). In this study, SbF_6^- is used as counteranion and dichloromethane (DCM) as solvent unless indicated otherwise (see Experimental Section). The two copper ions in **1** differ in coordination number and geometry, Figure 2a

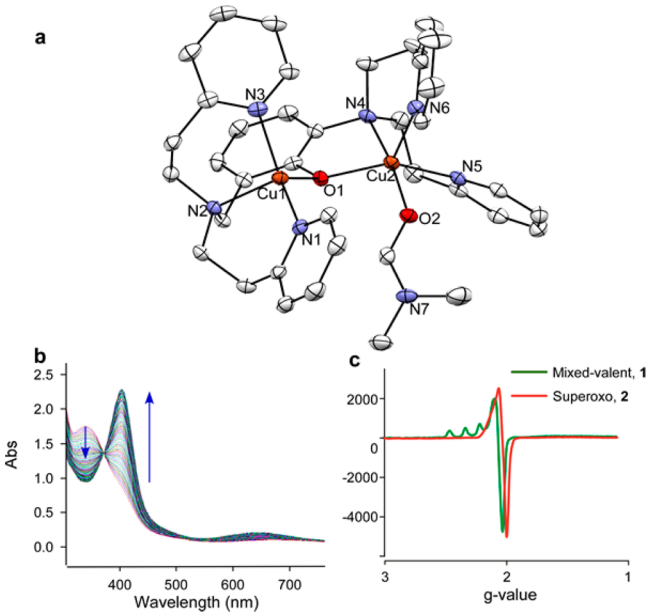

Figure 2. Displacement ellipsoid plot of **1**, its Oxygenation Reaction and EPR Spectroscopy. (a) Displacement ellipsoid plot (50% probability level) of the cationic part of the mixed-valent complex $[Cu^{I}Cu^{II}(UN\text{-}O^{-})(DMF)]^{2+}$ (**1**) at 110(2) K, Cu–Cu = 3.65 Å, hydrogen atoms are omitted for clarity. (b) UV–vis spectral changes due to the formation of superoxide complex $[Cu^{II}_{2}(UN\text{-}O^{-})(O_2^{\bullet-})]^{2+}$ (**2**) (λ_{max} = 404 nm) by oxygenation of **1** (λ_{max} = 350 nm) in DCM solution at −80 °C; time period ∼1 h. (c) Frozen DCM solution (∼77 K) EPR spectra of **1** and **2** (∼9 GHz). Also, see the text.

(and see the Supporting Information (SI) for further structural details). Cu1 (Figure 2a) is assigned as the cuprous ion based on its lower coordination number and a Bond Valence Sum Analysis (BVSA, see the SI).[10] Cu2 is the oxidized cupric ion (also from BVSA) which is pentacoordinate with a distorted square pyramidal geometry, with τ = 0.39 (τ = 1.0 for trigonal bipyramidal and τ = 0.0 for perfect square pyramidal coordination).[11] The DMF is coordinated to Cu2 via its carbonyl O atom (O2), Figure 2a. The Cu^{I}–Cu^{II} distance in **1** is found to be 3.65 Å.

The X-ray determined structure with its unsymmetrical nature and assignment of copper ion oxidation states puts complex **1** into the category of a Robin–Day Class I (localized) mixed-valent $Cu^{I}Cu^{II}$ complex.[12] We can conclude that the structure of $[Cu^{I}Cu^{II}(UN\text{-}O^{-})(DMF)]^{2+}$ (**1**) is maintained in solution based on the observation of a typical (for a single Cu ion) four line Cu^{II} (I = 3/2) electron paramagnetic resonance (EPR) spectrum (Figure 2c) with $g_{\|}$ = 2.25 at 77 K as previously reported.[8]

Oxygenation of 1, Giving Superoxide Complex $[Cu^{II}_{2}(UN\text{-}O^{-})(O_2^{\bullet-})]^{2+}$ (2). Formation of the superoxide $\mathbf{2}^{1,1}$ and $\mathbf{2}^{1,2}$, where the two are in fast equilibrium based on mixed-isotope resonance Raman spectroscopic and DFT analysis (vide infra), can be achieved by directly injecting excess dioxygen into complex **1** solution at −80 °C which is evident by formation of its distinct UV–vis absorption bands at 404 nm (5400 M^{-1} cm^{-1}) and 635 nm (670 M^{-1} cm^{-1}) (Figure 2b). The superoxide species $\mathbf{2}^{1,1}$ and $\mathbf{2}^{1,2}$ mixture gives an EPR spectrum which whose fine-structure could not be resolved, with a g value close to 2.0 (Figure 2c), with no indication for coupling to copper ions. This indicates that the unpaired electron is localized at the superoxide $O_2^{\bullet-}$ center (S = 1/2 as ground state), as previously described.[8]

Kinetic data for oxygenation of $[Cu^{I}Cu^{II}(UN\text{-}O^{-})]^{2+}$ (**1**) in DCM could be collected with benchtop UV–vis spectroscopy (Figure 2b). A second-order rate constant k_{on} has been calculated to be 9×10^{-2} M^{-1} s^{-1} (−80 °C, 193 K) (Table 1) based on k_{obs} data (see SI) and using the value $[O_2]$ = 2.0 mM for oxygen saturated DCM solution at −80 °C.[13] Activation parameters could also be determined (Table 1), see SI (Figure S4) for the Eyring plot.[14] The low-temperature rate constants for oxygenation of **1**, k_{on}, is small compared to many other ligand-Cu^{I}/O_2 reaction systems like those where TMPA, PV-TMPA, TMG_3tren, Me_6tren and $HIPT_3$tren (Table 1 and Figure S1) are all tripodal tetradentate N_4 ligands. All except $HIPT_3$tren are good donors and there is good steric access to the copper ion center; thus, the rate constants are very large, greater than 10^5 M^{-1} s^{-1}. The O_2-reaction with $[(Me_6tren)Cu^{I}]^{+}$ is slower because the solvent used was propionitrile, which is known to strongly compete with O_2 binding to the cuprous ion.[15] Reactions with the tridentate ligand-Cu(I) complexes (ligands, L^{iPr})[16] or the bidentate ligand-Cu(I) complex (L, HMe_2L^{iPr2}, a monoanion)[17] are quite slow (Table 1), probably also for reasons of steric access to the copper ion, see drawings of the ligands in the SI (Figure S1).

A contrasting reaction is the oxygenation of the dicopper(I) complex $[Cu^{I}_{2}(XYL\text{-}O^{-})]^{+}$ with dioxygen, involving a two-copper two-electron O_2-reduction to the peroxide dicopper(II) complex $[Cu^{II}_{2}(XYL\text{-}O^{-})(O_2^{2-})]^{+}$, which is exceedingly fast, too fast to be measured by stopped-flow kinetics-spectroscopy even at 193 K. This result is mentioned and tabulated here, because of the close analogy of the ligands XYL-O^- and UN-O^-, the former being a symmetric analogue of the latter (Figure S1).[13]

rRaman (rR) and DFT Analysis of Complex $[Cu^{II}_{2}(UN\text{-}O^{-})(O_2^{\bullet-})]^{2+}$ (2) Conformations. Laser excitation of frozen solutions of the superoxo complex **2**, consisting of $\mathbf{2}^{1,1}$ and $\mathbf{2}^{1,2}$ (vide infra) at 407 nm yield rR spectra that confirm the presence of a copper superoxide complex (Figure 3a, bottom). The presence of two oxygen isotope sensitive features (1144 cm^{-1} $\Delta^{18}O_2$ = −61 and 1120 cm^{-1} $\Delta^{18}O_2$ = −65 cm^{-1}) corresponds to two superoxide O–O stretches indicating the presence of two, distinct superoxide isomers. Additionally, two oxygen isotope sensitive Cu–O stretches are observed at lower energy (478 cm^{-1} $\Delta^{18}O_2$ = −22 and 383 cm^{-1} $\Delta^{18}O_2$ = −26 cm^{-1}, note the $^{18}O_2$ feature at 367 cm^{-1} is split into two features due to a Fermi resonance). Experimental evidence to distinguish between potential superoxide binding modes (μ-1,1- vs μ-1,2-) in **2** could be obtained from preparing rR samples with mixed isotope dioxygen (a 1:2:1 statistical mixture of $^{16}O_2$:$^{16,18}O_2$:$^{18}O_2$). This

DOI: 10.1021/jacs.6b02404
J. Am. Chem. Soc. 2016, 138, 7055–7066

Table 1. Kinetic Parameters for Selected Ligand-Copper (LCu_n^I) Frameworks Leading to 1:1 Cu^{II}_n-(O_2) Adducts (n = 1, 2)

ligand	solvent	k_{on} (M^{-1} s^{-1}), temp	$\Delta H^{\ddagger}$: kJ mol^{-1} $\Delta S^{\ddagger}$: J K^{-1} mol^{-1}	ref
UN-O^{-}[a]	DCM	$9.0 \pm 0.2 \times 10^{-2}$, 193 K	31.1 ± 1.1 -99 ± 6	this work
XYL-O^{-}[b]	DCM	$>1 \times 10^{6}$, 193 K		13
TMPA[c]	THF	$1.5 \pm 0.1 \times 10^{8}$, 193 K	7.62 −45.1	18
PV-TMPA[c]	MeTHF	$6.6 \pm 3.5 \times 10^{5}$, 193 K	9 ± 1 -97 ± 7	14
TMG_3tren[c]	MeTHF	$2.1 \pm 1.0 \times 10^{6}$, 193 K	10 ± 6 -70 ± 26	14
Me_6Tren[c]	EtCN	$9.5 \pm 0.4 \times 10^{4}$, 183 K	17.0 ± 0.2 -68 ± 0.9	15
$HIPT_3$tren[c]	acetone	2.3 ± 0.2, 183 K		19
L^{iPr}[c]	THF	7.6 ± 0.2 x10^{-1}, 183 K	24.4 ± 1.3 -110 ± 7	16
HMe_2L^{iPr2}[c]	THF	1560 ± 19, 223 K	18 ± 2 -100 ± 10	17

[a]Binucleating ligand one electron reduced copper−oxygen adduct Cu^{II}_2-($O_2^{\bullet-}$). [b]Binucleating ligand two electron reduced copper−oxygen adduct Cu^{II}_2-(O_2^{2-}). [c]Mononucleating ligand one electron reduced copper−oxygen adduct Cu^{II}-($O_2^{\bullet-}$). See SI, Figure S1 for drawings and full IUPAC names of the ligands.

spectrum (green, Figure 3a, top) does not indicate the presence of an intermediate Cu−O stretch (Figure 3a, top and Figure S7). As for the analysis of an end-on bound superoxo-copper(II) mononuclear complex,[20] these considerations indicate that the observed Cu−O vibrations originate from μ-1,1-superoxide isomers since only a single oxygen atom is coordinated to both Cu(II) ions. In contrast, the mixed isotope sample of a μ-1,2-isomer would yield a Cu−O stretch with energy approximately half way between the corresponding $^{16}O_2$ and $^{18}O_2$ vibrations since both oxygen atoms are coordinated to the Cu(II) ions.

Insight into the origin of the multiple superoxide isomers observed in the rR spectra was determined from a comparison of the ligand geometry over a number of new crystal structures containing the UN-O^- dicopper framework; $[Cu^{II}_2(^{NO2}UN\text{-}O^-)(Cl)]^{2+}$ and $[Cu^{II}_2(UN\text{-}O^-)(OH)]^{2+}$ possess a phenolato O atom bridge, plus either a μ-chloride or μ-hydroxide anion. (see SI, Figure S2−S3). In these complexes (Figure S7), the UN-O^- ligand adopts a number of different conformations depending on the crystallization conditions and the anion coordinating to the copper. To gather additional insights into the structure of **2**, density functional theory (DFT) calculations were performed on a number of these ligand conformations (Figure S8). A number of μ-1,1-superoxide isomers were found to have a similar energy and Cu···Cu distances in the range of 3.27−3.28 Å, very reasonable for a single atom bridging the two copper(II) ions, as the same Cu···Cu distance is observed for the structural analogues μ-chloride complexes 3.25 Å (see the SI). The computed O−O stretching frequencies of the isomers are predicted to be within 10 cm^{-1} of each other. Thus, due to the large experimental difference between the observed O−O frequencies (24 cm^{-1}), the solution likely also has a different type of isomer, a μ-1,2-superoxo form.

As a result, we considered the possibility of a μ-1,2-superoxide species being present in solution. DFT calculations of a μ-1,2-isomer (Table S4−S6) indicate a number of potential structures with a similar energy (all of the isomers in Tables S3−S6 are within 5 kcal/mol of each other) and Cu···Cu distances average about 3.47 Å (Table S4−S6). In addition, the O−O stretch of the μ-1,2-isomers are predicted to be similar and ∼25 cm^{-1} higher than the O−O stretch of the μ-1,1-isomers, in good agreement with the experimental data, and also supporting the results above. Hence, these calculations are able to reproduce two sets of O−O stretching frequencies that experimentally differ by 24 cm^{-1} being a mixture of μ-1,1- and a μ-1,2-superoxide isomers. From these structures, the observed rRaman features can be assigned where the 1144 cm^{-1} feature corresponds to the O−O stretch of the μ-1,2-isomer while the 1120 cm^{-1} stretch results from the μ-1,1-isomer. From the mixed isotope spectrum, the 478 and 383 cm^{-1} features must result from the μ-1,1-isomer and correspond to symmetric and antisymmetric Cu−O stretching frequencies (Table S7−S8).[21] DFT calculations also indicate that a transition state with a low barrier (less than or equal to 5 kcal/mol) connects these two superoxide-dicopper(II) structural isomers (Table S9), suggesting that they are able to rapidly interconvert in solution. Another line of supporting evidence comes from when the superoxide **2** rR samples are prepared from oxidation of the peroxide **3** using one equivalent of $AgSbF_6$. Then, the same spectrum containing both $\mathbf{2}^{1,1}$ and $\mathbf{2}^{1,2}$ are recorded. Since the oxidation of **3** would directly generate $\mathbf{2}^{1,2}$ (vide infra), the additional presence of $\mathbf{2}^{1,1}$ proves that the two isomers are interconvertible, in agreement with DFT predictions.

rRaman and DFT Analysis of Complex 3 Conformations. The peroxide species $[Cu^{II}_2(UN\text{-}O^-)(O_2^{2-})]^+$ (**3**) can be generated by direct oxygenation of the (LCu^I_2) species through injecting excess oxygen to the copper DCM solution at −80 °C, which has characteristic UV−vis absorption at 392 nm (3400 M^{-1} cm^{-1}), 510 nm (5300 M^{-1} cm^{-1}), 642 nm (2700 M^{-1} cm^{-1}). The peroxide complex **3** is also prepared by reduction of the superoxide complex **2** with one equivalent of decamethylferrocene (vide infra). The two sets of samples give rise to the same rRaman spectra.

Laser excitation of samples of **3** at 530 nm yield rR spectra that confirm the presence of a dicopper peroxo complexes (Figure 3b). The presence of multiple peroxide O−O stretches and more

DOI: 10.1021/jacs.6b02404
J. Am. Chem. Soc. 2016, 138, 7055−7066

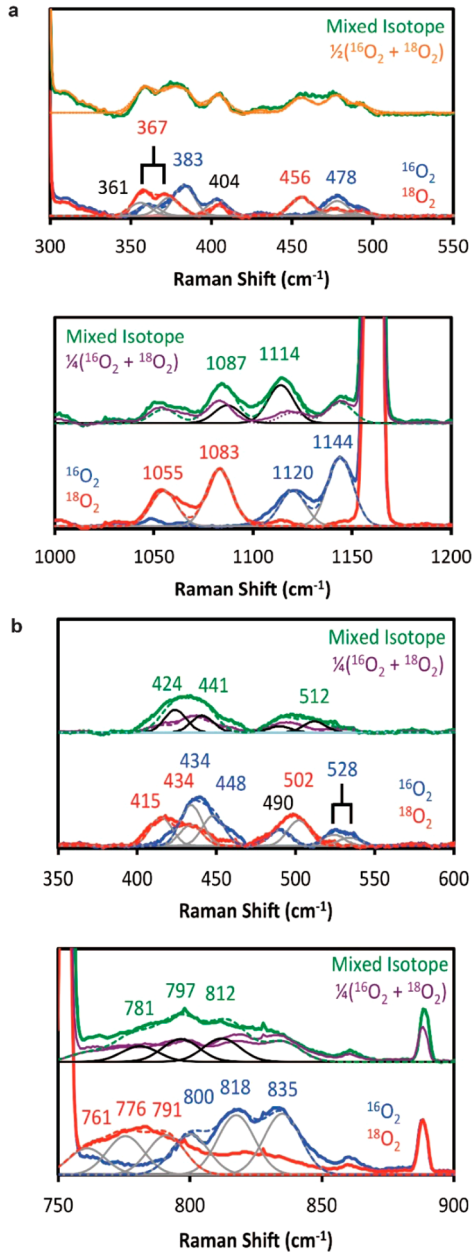

Figure 3. (a) Resonance Raman spectra of **2** with 407 nm excitation; $^{16}O_2$ (blue), $^{18}O_2$ (red), mixed isotope (a 1:2:1 mixture of $^{16}O_2$:$^{16,18}O_2$:$^{18}O_2$ green), 1/4($^{16}O_2$ + $^{18}O_2$) (purple), and 1/2($^{16}O_2$ + $^{18}O_2$) (orange) and Gaussian fits (individual transitions are gray for $^{16}O_2$ and $^{18}O_2$ and black for mixed isotope while the Gaussian sum for each spectrum is shown as a dashed curve). (b) Resonance Raman spectra of **3** with 530 nm excitation; $^{16}O_2$ (blue), $^{18}O_2$ (red), mixed isotope (a 1:2:1 mixture of $^{16}O_2$:$^{16,18}O_2$:$^{18}O_2$ green), and 1/4($^{16}O_2$ + $^{18}O_2$) (purple) and Gaussian fits (individual transitions are gray for $^{16}O_2$ and $^{18}O_2$ and black for mixed isotope while the Gaussian sum for each spectrum is shown as a dashed curve).

than two Cu−O stretches indicate multiple distinct isomers are present in solution. Laser excitation at 568 nm indicates that the three bands in the $^{16}O_2$ spectrum vary with excitation energy and are best fit by three, distinct Gaussians (Figure S9). Similarly, information about the geometry of **3** can be determined from the mixed isotope rR spectrum. For **3**, an intermediate Cu−O stretch with an intermediate frequency, that occurs in between the pure Cu−^{16}O and Cu−^{18}O vibrations (given by the purple average), is observed for each Cu−O stretch, indicating that these vibrations result from μ-1,2-peroxo isomers.

Additional insights into the structures of **3** can be obtained from DFT calculations on the various ligand conformations of UN-O$^-$ (Figure S8). A number of μ-1,2-peroxo isomers are found to have a similar energy (Table S10−S12) which vary by 28 cm^{-1} across the range of the isomers, in reasonable agreement with the experimental data which exhibits several closely spaced spectral features (Figure 3b, bottom). Attempts to compute the possible μ-1,1-peroxo isomers yielded structures of a mixed valent complex coordinated by a superoxide ion (Table S13). Therefore, one can conclude that the absence of an oxygen isotope sensitive vibration corresponding to a superoxide O−O stretch and the intermediate Cu−O stretches observed in the mixed isotope spectrum indicate that the structure of **3** is best described by three μ-1,2-peroxo conformational isomers. It should also be noted that the calculated DFT structures give a Cu···Cu distance averaging 3.44 Å (Tables S10−S12); this is in reasonable agreement with an older EXAFS-derived value (but on an isolated solid) of ∼3.3 Å.[9a]

Chemical Interconversion of Species [Cu$^{II}_2$(UN-O$^-$)-(O$_2^{\bullet-}$)]$^{2+}$ (2) and [Cu$^{II}_2$(UN-O$^-$)(O$_2^{2-}$)]$^+$ (3); Reduction Potential Determination. As mentioned in the introduction, superoxide and peroxide complexes **2** and **3** are interconvertible. These reactions can be carried out using a series of ferrocene or ferrocenium derivatives, in DCM as solvent, Figure 4a.[22] With deca- or octa-methyl ferrocene, a titration can be carried out, showing that only one equiv of reductant is required to fully convert superoxide complex **2** to peroxide complex **3**, Figure S5b. For the opposite reaction, addition of one equiv ferrocenium hexafluoroantimonate derivatives (the parent unsubstituted ferrocenium salt, and either acetyl or dimethyl ferrocenium) to solutions of peroxide complex **3** results in complete oxidation of the peroxide complex to superoxide species **2**. Such a titration (adding 1/4 equiv oxidant for each recorded spectrum) is shown in Figure 4b, for dimethylferrocenium as oxidant. Following completion of this reaction, readdition of 1 equiv decamethylferrocene reductant gave back the peroxo complex **3** in 90% yield (−80 °C, as determined from spectrophotometry, see Figure S5b). In either direction of the reaction, the transformations are consistently fast; i.e., the reactions were complete immediately following benchtop addition of the redox reagent and recording of UV−vis spectrum, suggesting that an outer-sphere electron transfer mechanism is operative.

By choosing the right oxidizing reagent, in particular diphenylamine ferrocenium (Figure 4a) we could achieve an equilibrium condition, where all oxidant and reductant pairs are present in amounts that could be quantified by spectrophotometry. This oxidant possesses a formal reduction potential close to that of the superoxide(**2**)/peroxide(**3**) pair, in fact, complex [Cu$^{II}_2$(UN-O$^-$)(O$_2^{\bullet-}$)]$^{2+}$ (**2**) is present in greater amounts than peroxide species [Cu$^{II}_2$(UN-O$^-$)(O$_2^{2-}$)]$^+$ (**3**); most but not all of peroxide species **3** becomes oxidized, Figure 4c. The amount of diphenylamine ferrocenium ion present can be directly quantitated by its known absorption at 1014 nm (ε = 2675 M^{-1} cm^{-1}) (Figure 4c and SI). The Nernst equation (eq 3) could be directly applied to this system which is at equilibrium, as λ_{max} and absorptivity (ε) values are known for both **2** and **3**; by direct measurement of the concentration of diphenylamine ferrocenium, the amount of diphenylferrocene was determined by difference. Thus, the electron-transfer equilibrium constant (K_{et}) was determined to be K_{et} = 5.3.[23] By employing this value along with our experimentally measured reduction potential of

DOI: 10.1021/jacs.6b02404
J. Am. Chem. Soc. 2016, 138, 7055−7066

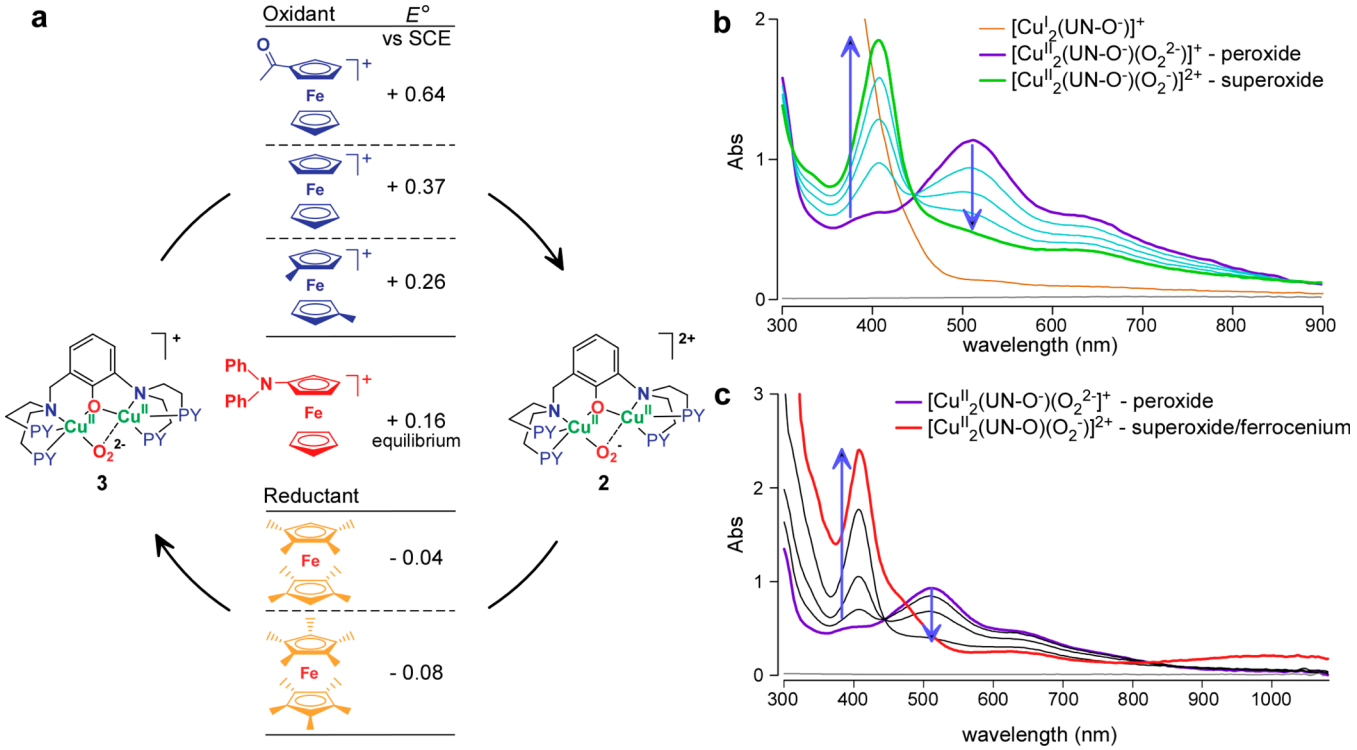

Figure 4. UV−vis spectroscopy of the $[Cu^{II}_2(UN\text{-}O^-)(O_2^{2-})]^+$ (**3**) and $[Cu^{II}_2(UN\text{-}O^-)(O_2^{\bullet-})]^{2+}$ (**2**) interconversion as well as equilibrium for **3** converting to **2** with diphenylamine ferrocenium as oxidant. (a) $E°$ values for the oxidants used to convert **3** to **2** and for the reductants used to convert **2** to **3**. (b) Oxidation of **3** to **2** using dimethylferrocenium ion. (c) Diphenylamine ferrocenium as oxidant used to reach an equilibrium state between **3** and **2**.

the diphenylamine ferrocenium/ferrocene pair, the $E°$ value for the superoxide/peroxide (**2**/**3**) pair is calculated to be +130 mV vs SCE.[23]

$$E(\mathbf{3}/\mathbf{2}) = E_{ox} + (RT/F)\ln K_{et} \quad (3)$$

or

$$0 = E°_{et} - \frac{RT}{nF}\ln K_{et},$$

$$E°_{et} = E°\left(\frac{Ph_2NFc^+}{Ph_2NFc}\right) - E°\left(\frac{Superoxide}{Peroxide}\right)$$

***E°* for Reduction of 2 to 3 and Comparisons to Other Systems.** Given that this is the first determination of a copper coordinated dioxygen-derived fragment reduction potential (eq 4; $E°$ = +130 mV vs SCE), comparison to the literature is constructive.

$$[Cu^{II}_2(UN\text{-}O^-)(O_2^{\bullet-})]^{2+}(\mathbf{2}) + e^- \rightarrow [Cu^{II}_2(UN\text{-}O^-)(O_2^{2-})]^+(\mathbf{3}) \qquad E° = +0.13V \quad (4)$$

Perhaps closely related comparisons can be made with the well-known superoxo- and peroxo-bridged dicobalt(III) complexes. One example comes from complexes employing a phenolato-bridged binucleating ligand pbpb$^-$ ((2,6-bis(*N*,*N*-bis(2-pyridyl-methyl)aminomethyl)-4-*tert*-butylphenolate)),[24] somewhat similar to our own UN-O$^-$ ligand (Table 2). Superoxo-to-peroxo dicobalt(III) complex reduction potentials (see Table 2 (in acetone vs SCE)) are far more positive (i.e., favorable). Likely this is due to the higher charged cobalt(III) ion, compared to copper(II). It should be noted that one cannot generally compare standard reduction potentials ($E°$) in different solvents; however, for potentials measured for the ferrocenium/ferrocene (Fc^+/Fc) couple,[22,25] and $E°$ values determined for a variety of other kinds of organic or inorganic compounds that are electrochemically active, there are only quite small differences in the $E°$ value in DCM vs acetonitrile (ACN) vs acetone vs dimethylformamide (DMF).[26]

Within this dicobalt set, the complex supported by a better donor ancillary ligand, acetate compared to trichloroacetate, leads to a less favorable superoxide-to-peroxide reduction. The better donor would destabilize (in a relative sense) reductive conversion to the more negatively charged dianionic peroxide ligand; conversely the trichloroacetate ligand can help stabilize some of the extra negative charge of the peroxide complex.

Data on other dicobalt(III) complexes also reveal interesting findings. For the classical dicobalt(III) compound with a single bridging superoxide ligand, $[Co_2(NH_3)_{10}(\mu\text{-}O_2^{\bullet-})]^{5+}$, the reduction potential is over 300 mV more oxidizing than the closely related doubly bridged complex $[Co_2(NH_3)_8(\mu\text{-}O_2^{\bullet-},NH_2)]^{4+}$ (Table 2), likely because of the difference in overall charge of the complexes. Still, both these complexes and that dicobalt compound with the pbpb$^-$ ligand containing species (see discussion above) have $E°$ values significantly more positive than that for our $[Cu^{II}_2(UN\text{-}O^-)(O_2^{\bullet-})]^{2+}$ (**2**)/$[Cu^{II}_2(UN\text{-}O^-)(O_2^{2-})]^+$ (**3**) redox couple (Table 2). The grossly more negative $E°$ value for $[Co_2(CN)_{10}(\mu\text{-}O_2^{\bullet-})]^{5-}$, is ~900 mV less oxidizing than the ammonia ligand containing analogue, the explanation for this observation being that the complex has a vastly altered overall charge of 5−.[27a]

Interestingly, recent synthetic advances allowed for the stabilization of three peroxide dianion moieties, by using various organic "hosts".[28,33,34] For two of these, superoxide-to-peroxide

DOI: 10.1021/jacs.6b02404
J. Am. Chem. Soc. 2016, 138, 7055−7066

Table 2. List of Redox Pairs of Interest for Comparisons

redox pair	n^a	solvent	E° (mV) vs SCE	ref
$[Co_2(bpbp^-)(CCl_3CO_2^-)(O_2^{\bullet-})]^{3+}$ / $[Co_2(bpbp^-)(CCl_3CO_2^-)(O_2^{2-})]^{2+}$	1	Acetone	1060	24
$[Co_2(bpbp^-)(CH_3CO_2^-)(O_2^{\bullet-})]^{3+}$ / $[Co_2(bpbp^-)(CH_3CO_2^-)(O_2^{2-})]^{2+}$	1	Acetone	880	24
$[Co_2(NH_3)_{10}(\mu\text{-}O_2^{\bullet-})]^{5+}$ / $[Co_2(NH_3)_{10}(\mu\text{-}O_2^{2-})]^{4+}$	1	Water	708[b]	27
$[(C_6F_5)_3B]_2O_2^-$ / $[(C_6F_5)_3B]_2O_2^{2-}$	1	DCM	540	28
Fc^+/Fc	1	DCM	370	22
$[Co_2(NH_3)_8(\mu\text{-}O_2^{\bullet-}, NH_2)]^{4+}$ / $[Co_2(NH_3)_8(\mu\text{-}O_2^{2-}, NH_2)]^{3+}$	1	Water	358	27
Me_2Fc^+/Me_2Fc	1	DCM	260	this work
(**2**)/(**3**)	1	DCM	130	this work
Cyt *c*	1	ACN	3	29
$iAscH^{\bullet-}/iAscH^-$	1	ACN	−30	30
$[HTrip\cdots O_2] + 2H^+$ / $[HTrip + H_2O_2]$	2	PhCN	$-40 < E^\circ < 260$	31
$TMG_3trenCu^{II}(O_2^{\bullet-}) + H^+$ / $TMG_3trenCu^{II}OOH$	1	MeTHF	$-40 < E^\circ < 260$	32
Me_8Fc^+/Me_8Fc	1	DCM	−40	this work
$Me_{10}Fc^+/Me_{10}Fc$	1	DCM	−80	this work
$[Co_2(CN)_{10}(\mu\text{-}O_2^{\bullet-})]^{5-}$ / $[Co_2(CN)_{10}(\mu\text{-}O_2^{\bullet-})]^{6-}$	1	Water	−182	27
$[(O_2^{\bullet-}) \subset mBDCA\text{-}5t\text{-}H_6]^-$ / $[(O_2^{2-}) \subset mBDCA\text{-}5t\text{-}H_6]^{2-}$	1	DMF	−520	33

[a]Number of electrons. [b]Value determined at neutral pH; for pH < 1 $E^\circ \sim 470$ mV vs SCE. $iAscH^{\bullet-}$; as 5,6-isopropylidiene ascorbyl anion/radical. Cyt *c*; Cytochrome *c*. HTrip; [14]triphyrin(2.1.1). TMG_3tren; see Figure S1. mBDCA-5t-H_6; *tert*-butyl-substituted hexacarboxamide cryptand.

reduction potentials were obtained by cyclic voltammetry (CV), see Table 2. In one example by Agapie and co-workers[28] the O_2^{2-} fragment was captured by $B(C_6F_5)_3$ as a Lewis acid, giving the species $[(C_6F_5)_3B{-}O{-}O{-}B(C_6F_5)_3]^{2-}$: a quasi-reversible oxidation wave (CV) occurred at +0.54 V vs SCE (Table 2). By comparison, this is more than 400 mV higher than that found for our complex with superoxide or peroxide are dicopper(II) coordinated. This may be ascribed to the very strong Lewis acidity of the $B(C_6F_5)_3$ moieties. Another example is provided by Cummins, Nocera and co-workers[33] where corresponding superoxide or peroxide moieties are encapsulated in a hexacarboxamide cryptand through hydrogen bonding networks. A standard reduction potential measured in this case, in DMF solvent is $E^\circ = -520$ mV vs SCE. Solvent variations in E° or not, this value is quite low compared to the (**2**)/(**3**) couple; apparently the extensive cryptand H-bonding is sufficient to stabilize the O_2^{2-} fragment, but it is not nearly as effective as our dicopper(II) or the $B(C_6F_5)_3$ bound peroxide.

In further comparison, we previously were able to bracket the reduction potential associated with a protonated superoxo species, $TMG_3trenCu^{II}(O_2^{\bullet-})H^+$ conversion to the corresponding hydroperoxide complex $TMG_3trenCu^{II}OOH$, Table 2, to be found within the range between Me_2Fc^+/Me_2Fc and Me_8Fc^+/Me_8Fc. Notably, the same is true for our $[Cu^{II}_2(UN\text{-}O^-)(O_2^{\bullet-})]^{2+}$ (**2**)/$[Cu^{II}_2(UN\text{-}O^-)(O_2^{2-})]^+$ (**3**) couple. Also worth mentioning is a recent study by Fukuzumi and co-workers[31] where they bracketed the two-electron two-proton reduction potentials of O_2 in the presence of an organic macrocycle Htrip and $HClO_4$ to also fall in the range between Me_2Fc and Me_8Fc reagents (Table 2).

To further put our results (eq 4) and the others carried out in organic solvents (discussed just above) in context, we can compare to E° values for biologically relevant reductants, those determined in ACN solvent. The heme protein cytochrome *c* and an organic soluble ascorbate analogue also possess standard reduction potentials that lie between those of the Me_2Fc^+/Me_2Fc and Me_8Fc^+/Me_8Fc couples (Table 2). We can conclude, that our study and the others, do possess biological relevance, in that the reduction potentials lie in a range within or close to those occurring in biochemistry; perhaps, cytochrome *c* or ascorbate could reduce $[Cu^{II}_2(UN\text{-}O^-)(O_2^{\bullet-})]^{2+}$ (**2**) to $[Cu^{II}_2(UN\text{-}O^-)(O_2^{2-})]^+$ (**3**). We extend the argument to say that our work with copper or dicopper bound O_2-derived reduced fragments can and will provide useful if not important information in the biological context.

Also, it is well-known and clear from literature data that there is a considerable importance for the role of protons in the reduction of O_2-derived fragments. Protonation and formation of very strong O−H bonds greatly enhances reactions (i.e., protons usually accompany electrons). For example, the addition of an electron to the P450 monoxygenase heme-superoxo (i.e., $Fe^{III}{-}O_2^{\bullet-}$) species, a neutral entity, to give the corresponding reduced

DOI: 10.1021/jacs.6b02404
J. Am. Chem. Soc. 2016, 138, 7055−7066

peroxide anion, is extremely uphill, eq 5.[5b] The process switches over to being highly favorable if a proton is involved, eq 6 at pH 7.0.[35]

$$\mathrm{P450{-}Fe^{III}(O_2^{\bullet-})^{2+}} + \mathrm{e^-} \rightarrow \mathrm{P450{-}Fe(O_2^{2-})^{+}} \qquad E^{\circ\prime} \leq -1.0\mathrm{V} \tag{5}$$

$$\mathrm{P450{-}Fe(O_2^{\bullet-})^{2+}} + \mathrm{H^+} + \mathrm{e^-} \rightarrow \mathrm{P450{-}Fe(^{-}OOH)^{2+}} \qquad E^{\circ\prime} = +0.80\mathrm{V\ (vs\ SCE)} \tag{6}$$

It will be of considerable future interest to determine the thermodynamics for the reduction *and* protonation of $[Cu^{II}_2(UN\text{-}O^-)(O_2^{\bullet-})]^{2+}$ (**2**) to give the hydroperoxide complex $[Cu^{II}_2(UN\text{-}O^-)(^{-}OOH)]^{2+}$; the latter has been separately characterized and is known to have a μ-1,1-hydroperoxo structure.[36] Knowledge of such thermodynamic parameters would be of interest in comparing with the values in eqs 5 and 6 or other known cases.[4,5b,35]

Electron-Transfer Oxidation of Peroxo Species $[Cu^{II}_2(UN\text{-}O^-)(O_2^{2-})]^+$ (3) to Give Superoxo Complex $[Cu^{II}_2(UN\text{-}O^-)(O_2^{\bullet-})]^{2+}$ (2). Stopped-Flow Kinetics. In order to obtain further mechanistic insights, the electron-transfer kinetics of the oxidation of peroxo complex **3** by the dimethylferrocenium ion (Me_2Fc^+) were followed by the low-temperature (−80 °C) stopped-flow method. With an excess of Me_2Fc^+ (i.e., under pseudo-first-order conditions) the oxidation of the peroxide **3** is too fast to observe instrumentally. Therefore, we employed a one-to-one ratio for the peroxide **3** and dimethylferrocenium at low concentration to observe the second-order decay of the peroxide-to-superoxide **3** → **2** (as from eq 7); an example of the data obtained is shown in Figure 5 and k_{et} values could be determined from a plot of $[\mathbf{3}]^{-1}$ vs time (Table 3).

$$\mathrm{d}[\mathbf{3}]/\mathrm{d}t = -k_{et}[\mathbf{3}]^2 \tag{7}$$

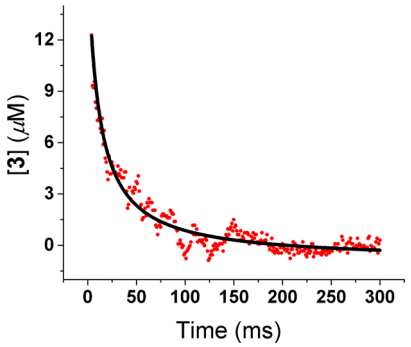

Figure 5. Time course for the electron transfer from **3** to Me2Fc$^+$ to produce **2** in DCM solvent at −80 °C.

Calculation of the Reorganization Energy λ. Using k_{et} values determined as above, and given in Table 3 at various temperatures, a plot of ln k_{et} vs T^{-1} (Figure 6) gives rise to activation free enthalpy and entropy values (eq 8) for the conversion peroxide-to-superoxide (**3** + Me_2Fc^+ → **2**[1,2] + Me_2Fc), $\Delta H^{\ddagger}$ = (17 ± 3) kJ mol^{-1} and $\Delta S^{\ddagger}$ = (−16 ± 16) J K^{-1} mol^{-1}, respectively. According to the classic Marcus theory for

Table 3. Rate Constants for the Electron Transfer from 3 to Me_2Fc^+ Determined at Various Temperatures

T (°C)	k_{et} (M^{-1} s^{-1})
−55	(6.0 ± 2.0) · 10^7
−60	(3.3 ± 1.1) · 10^7
−65	(2.3 ± 1.2) · 10^7
−70	(2.2 ± 0.9) · 10^7
−75	(2.0 ± 0.8) · 10^7
−80	(1.2 ± 0.3) · 10^7

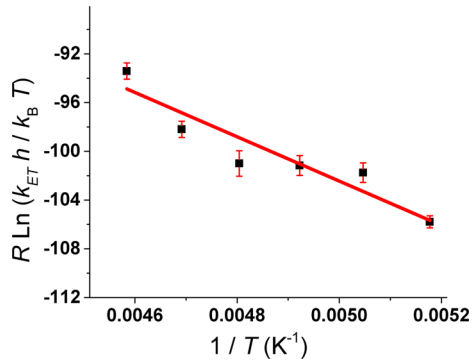

Figure 6. Plot of ln k_{et} vs T^{-1} for the electron transfer from $[Cu^{II}_2(UN\text{-}O^-)(O_2^{2-})]^+$ (**3**) to Me_2Fc^+ in DCM solvent.

intermolecular electron transfer,[37] the activation free energy, $\Delta G^{\ddagger}$, is given by eq 9,

$$\Delta G^{\ddagger} = \Delta H^{\ddagger} - T\Delta S^{\ddagger} \tag{8}$$

$$\Delta G^{\ddagger} = (\lambda + \Delta G^{\circ})^2/4\lambda \tag{9}$$

$$\Delta G^{\circ} = -nF[E^{\circ}(\mathrm{Me_2Fc^{+/0}}) - E^{\circ}((\mathbf{2})/(\mathbf{3})] = -12.5\ \mathrm{kJ/mol} \tag{10}$$

where ΔG° (eq 10) is the difference of the reduction potential of the dimethylferrocenium ion/dimethylferrocene couple (Me_2Fc^+/Me_2Fc = +260 mV vs SCE) and that of the superoxide/peroxide complexes **2**/**3** (+130 mV vs SCE). Then, the reorganization energy, λ, for the electron transfer is calculated to be 1.1 ± 0.2 eV (see diagram below); this is the first measurement of such a fundamentally important parameter for the redox chemistry of interconverting superoxide anion and peroxide dianion ligated to a dicopper(II) center.

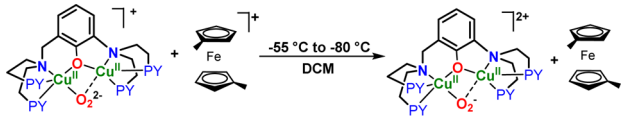

$\lambda = \lambda_{ET}$ = ***overall reorganization energy*** = 1.1 ± 0.2 eV

In order to further confirm the value mentioned above, the reorganization energy for the electron transfer was also estimated using eq 11, considering the second-order rate constant and the superoxo−peroxo reduction potential, both measured at −80 °C in this work:

$$k_{ET} = Z\exp[-(\lambda + \Delta G^{\circ})^2/4\lambda RT)] \tag{11}$$

where Z is the frequency factor, taken as 1×10^{11} M^{-1} s^{-1} at 298 K and ΔG° is from eq 10. The value found using this method is 0.84 ± 0.02 eV, which is consistent with 1.1 ± 0.2 eV.

DOI: 10.1021/jacs.6b02404
J. Am. Chem. Soc. 2016, 138, 7055−7066

This experimentally determined reorganization energy λ = 1.1 eV is the total reorganization energy of the system, composed of the average of the sum of the bond reorganization energies of the (Peroxide/Superoxide) and (Me_2Fc^+/Me_2Fc) pairs (λ_{inner}), plus the solvent reorganization energy (λ_{outer}).

The inner sphere reorganization energy for the electron transfer between the μ-1,2-superoxo and μ-1,2-peroxo isomers could be computed for each ligand conformation from DFT structures on superoxide $[Cu^{II}_2(UN\text{-}O^-)(O_2^{\bullet-})]^{2+}$ ($\mathbf{2^{1,2}}$) and $[Cu^{II}_2(UN\text{-}O^-)(O_2^{2-})]^+$ (**3**) complexes. A small inner sphere reorganization energy of ∼0.4 eV was predicted which results from the small geometric perturbation between the superoxo and peroxo structure of the complexes (see Table S15). Specifically, in the DFT optimized structures the peroxo O−O bond decreases from 1.356 to 1.293 Å in the superoxo complex (Δ_{O-O} = 0.063 Å) and there is an increase in the average Cu−O from 1.985 to 2.047 Å. This change is small compared to that calculated by DFT for oxidation of an isolated peroxide dianion, wherein the O−O distance decreases from 1.607 to 1.354 Å (Δ_{O-O} = 0.208 Å) yielding a λ_{inner} of 0.76 eV using identical methodology. (see Table S17)

To calibrate these calculations, the λ_{total} for Fc^+/Fc self-exchange was determined by DFT. This value serves as a useful benchmark for crosschecking our calculations because the value is well-known in the literature and is roughly invariant for a number of solvents such as acetone, acetonitrile and methanol.[36] First, λ_{inner} for Fc was calculated analogously as above, and was determined to be 0.102 eV which is reasonable considering the negligible change in structure upon oxidation of Fc, that seen from our calculations see SI (Table S16). Next, λ_{outer} was estimated using a dielectric continuum model (eq 12):[38]

$$\lambda_{outer} = (\Delta e)^2\left[\frac{1}{2a_1} + \frac{1}{2a_2} - \frac{1}{r}\right]\left[\frac{1}{D_{optical}} - \frac{1}{D_{static}}\right] \quad (12)$$

where the radius of ferrocene $a_1 = a_2$ = 0.406 nm, r = 0.812 nm, and $D_{optical}$ and D_{static} are defined as the optical and static dielectric constants of the solvent, which for acetonitrile are 1.806 and 37.5 respectively. This estimation yielded a λ_{outer} of 0.934 eV, for an overall λ_{total} of 1.036 eV. This value compares well to 1.06 eV measured experimentally in acetonitrile.[39]

To determine the λ_{outer} contribution to the ferrocenyl reduction of the superoxide dicopper complex in DCM, the dielectric continuum model was used again with the radius of **2** estimated to be 0.678 nm (calculated, see SI), ferrocene 0.406 nm, and the $D_{optical}$ and D_{static} of DCM as 2.03 and 9.08 which yielded a λ_{outer} of 0.56 eV. Thus, the calculations yielded a λ_{total} of 0.81 eV, which is in reasonable agreement with the Eyring plot derived value of 1.1 ± 0.2 eV, i.e., its lower side value (1.1−0.2 = 0.9 eV), but in excellent agreement with the value of 0.84 ± 0.02 eV derived from the experimentally determined electron transfer rate at −80 °C using eq 11.

Kinetic data on the electron-transfer reduction of some superoxo-dicobalt(III) complexes have also provided λ value information. Thus, for the $[Co_2(NH_3)_{10}(\mu\text{-}O_2^{\bullet-})]^{5+}$ (Table 2) reduction by the cobalt(II) outer-sphere reducing agent, $[Co(terpyridine)_2]^{2+}$[27a] or ascorbate,[40] λ_{total} values of 2.9 eV and ∼2.0 eV, respectively, could be determined from the cross-reaction rate constant and known thermodynamics for the redox partners involved. These reactions proceed reasonably fast with log k_{12} = 3−5 at RT for reactions with driving forces of ΔE = 0.5−0.7 V. While our detailed kinetic study is on the oxidation of $[Cu^{II}_2(UN\text{-}O^-)(O_2^{2-})]^+$ (**3**), when we carry out the reduction of superoxo complex $[Cu^{II}_2(UN\text{-}O^-)(O_2^{\bullet-})]^{2+}$ (**2**), with Me_8Fc, the reaction is very fast, immediate by benchtop observation, at −80 °C, where the thermodynamic driving force ΔE_{rx} is only ∼0.1 V. One can conclude that the reorganization energy for our dicopper superoxo/peroxo electron-transfer interconversion is far smaller than that for the dicobalt analogues. In support of this and perhaps a better comparison is that when $[Ru(bpy)_3]^{3+}{}_{(aq)}$ oxidizes $[Co_2(NH_3)_8(\mu\text{-}O_2^{2-}, NH_2)]^{3+}$ log k_{12} = −6 (RT, aqueous) where ΔE°_{rx} is ∼0.5 V.[41] Thus, a thermodynamically very favorable oxidation of the bridged dicobalt(III) peroxo compound is exceedingly slow when compared to our extremely fast analogous reaction involving copper, **3** + Me_2Fc^+ → $\mathbf{2^{1,2}}$ + Me_2Fc (at −80 °C); again, this is consistent with our finding of a very small λ_{total} (and λ_{inner}) for dicopper, but the presence of an unfavorable large reorganization energy for the dicobalt system.

Similarly, for an aqueous dirhodium[42] superoxide complex, $\{[(H_2O)_4(OH)Rh^{III}(O_2)Rh^{III}(OH)(H_2O)_4]^{3+}\}$,[41] reduction to its peroxide counterpart occurs with a large thermodynamic driving force (>1 V) when strong reducing agents such as $V^{2+}{}_{(aq)}$ and $Eu^{2+}{}_{(aq)}$ are elected, the reaction only shows moderately fast kinetics, log k_{12} ∼ 5. Therefore, a large reorganization energy is operative for the reduction of this dirhodium superoxo complex.

Cummins, Nocera and co-workers,[43] with their hexacarboxamide cryptand encapsulated peroxide or superoxide anion (see above), also determined a reorganization energy of 1.5 eV by using photoexcited ruthenium(II) complexes as oxidants for the conversion of the peroxide dianion to superoxide anion (eq 13).[43] The inner-sphere reorganization energy portion of that was determined to be 0.9 eV based on DFT calculations.

$$^-O\text{−}O^-\ (H-\text{bonding cryptand}) - e^- \rightarrow O\text{−}O^{\bullet-}\ (H-\text{bonding cryptand}) \quad (13)$$

It serves to be emphasized, that in the present study, the reorganization energy of the **2** → **3** transformation is small compared to the cryptand and isolated dianion, which suggests a sizable metal complex (i.e., dicopper) contribution in decreasing the magnitude of the reorganization. To elucidate the nature of the contributions, we analyzed the donation of the peroxide/superoxide to the copper in the frontier molecular orbitals using a Mullikan population analysis. The oxygen character in the unoccupied Cu orbitals (186α and 186β) were 42.2% and 44.9% in the peroxide complex, whereas in the superoxide complex, the O_2 π^* contributions were 34.4% and 11.1% (185β and 186α). Thus, the peroxide has a much greater π^* donation. This enhanced donation is reflected in the Mayer bond order, where the Cu−O bonds were 0.75 (average) in the peroxide compared to 0.517 (average) in the superoxide. (SI, Table S18) The average Cu−O bond lengths also increased from 1.985 Å in the peroxide to 2.047 Å in the superoxide, while the Cu−N distances slightly contracted. The significantly better covalency in the peroxide complex thus distributes the distortion over more centers, and as the reorganization energy goes by the square of the distortion,[38] by distribution the distortion over more centers the reorganization energy is dramatically lowered.

Thus, the low reorganization energy for reduction of superoxo complex $\mathbf{2^{1,2}}$ to peroxo species **3**, in fact experimentally determined by ferrocenium oxidations of **3**, occurs with no change in copper oxidation state, little if any change in the overall coordination geometry and only small changes in O−O and Cu−O bond distances. We can further compare the λ value of 1.1 eV with situations where complexes with Cu(II) are reduced to Cu(I). A λ value of 1.6 eV[44] is found for ferrocenyl (Me_2Fc and

DOI: 10.1021/jacs.6b02404
J. Am. Chem. Soc. 2016, 138, 7055−7066

Fc) reductions of the dicopper(II) complex $[Cu^{II}_2(N3)]^{4+}$ to its dicopper(I) analogue (N3 is a binucleating ligand possessing bis(2-pyridylethyl)amine (PY2) tridentate moieties connected by a $-(CH_2)_3-$ linker); the Cu(II) coordination environments include four or five ligand donors,[45] whereas the Cu(I) ligation to the PY2 tridentate moieties are three coordinate or sometimes a fourth exogenous ligand binds.[45a,46] With copper ion in a tetradentate tris(2-pyridylmethyl)-amine (tmpa) environment, the Cu(II) to Cu(I) reorganization energy is smaller, $\lambda = 1.29$ eV, also using ferrocenyl redox reagents, where both Cu(II) and Cu(I) tmpa complexes tend to be pentacoordinate with a solvent molecule as fifth ligand.[47]

Another value for comparison is $\lambda = 2.2$ eV found for the electron transfer from $Me_{10}Fc$ and Me_8Fc to the peroxo complex $[Cu^{II}_2(N3)(O_2^{2-})]^{2+}$.[44] This very large λ value has its origin in the fact that O−O bond cleavage occurs upon electron-transfer reduction. In contrast to this, for the electron-transfer reduction of $\mathbf{2}^{1,2}$ to **3**, no O−O cleavage occurs and a smallish change in O−O bond distance is expected, $O-O_{superoxide} \sim 1.29$ Å and $O-O_{peroxide} \sim 1.36$ Å. As mentioned above, the ferrocenyl reduction of $[Cu^{II}_2(UN\text{-}O^-)(O_2^{\bullet-})]^{2+}$ (**2**) to $[Cu^{II}_2(UN\text{-}O^-)(O_2^{2-})]^{+}$ (**3**) occurs with $\lambda = 1.1$ eV (experimentally derived) while the internal electron-transfer reorganization energy could be calculated to be ∼0.4 eV (vide supra).

As we are emphasizing metal-bound oxygen derived species, high-valent metal-oxo complexes are of great biological and chemical interest, as strong electron-transfer oxidants or oxygen-atom transfer reagents.[48] Heme-containing horseradish peroxidases effect electron-transfer oxidations when the active species generated are Compound I $[(P^{\bullet+})Fe^{IV}{=}O]$ or Compound II $[(P)Fe^{IV}{=}O]$ (where $P^{\bullet+}$ is a porphryinate radical cation); for these one-electron reduction reactions, reorganization energies have been calculated to be 1.3 and 1.6 eV, respectively.[49] A smaller λ value is associated with a more reactive species, i.e., the activation energy for reaction is lower, cf. eq 9. Some high-valent macrocycle-$Mn^{V}{=}O$ or $Mn^{IV}{=}O$ complexes have been shown to possess similar λ values, 1.5 and 1.7 eV respectively.[50] However, nonheme high-valent $Fe^{IV}{=}O$ complexes, important in biochemistry and in synthetic chemical systems, have higher reorganization energies for $Fe^{IV/III}$ transformations, in the range of 2.0 to 2.7 eV, due to a significantly greater flexibility of their supporting ligands.[48]

There is some data available for a dioxygen (molecular oxygen) reduction to superoxide anion reorganization energies. In aqueous media the total reorganization energy, λ, has been determined to be 1.97 eV.[51] In a calculation by Fukuzumi, based on thermodynamic data available, a $Cu^{I}-O_2$ species where dioxygen is hypothetically bound to copper(I) prior to electron-transfer), the internal (inner-sphere) electron-transfer from the copper(I) to the O_2 to give a cupric-superoxide product (that species which is observed) gives a calculated λ (total) value of 1.74 eV.[47b] A related calculation indicates that free dioxygen binds to a porphryinate-cobalt(II) complex to give the Co(III)-superoxide species with $\lambda = 1.89$ eV.[47b] An interesting finding and analysis by Roth and Klinman[52] is that for glucose oxidase, reduction of O_2 to give superoxide is rate-limiting but is made to be quite fast because of an enzyme adaption which lowers the reorganization energy by ∼0.8 eV, via generation of a positive charge from His protonation.

Again, to overview, this small λ value for the reduction of $[Cu^{II}_2(UN\text{-}O^-)(O_2^{\bullet-})]^{2+}$ (**2**) to $[Cu^{II}_2(UN\text{-}O^-)(O_2^{2-})]^{+}$ (**3**) may possess further biological relevance since low λ values are estimated in many enzyme catalyzed reactions.[53] In "blue" electron-transfer copper proteins, the copper ion ligand environment is essentially fixed for both copper ion oxidation states, in order for that biologically efficient redox chemistry to occur; λ values in such proteins are as low as 0.6 eV.[54] For the heme protein cytochrome *c*, Warshel and co-workers[53c] have estimated the solvent (water) reorganization to be between 0.4 to 0.65 eV and the protein contribution to be 0.35 to 0.45 eV. Gray and Winkler[53b] have made similar findings, and including still other redox proteins, low reorganization energies in the range of 0.5−1.2 eV exist.

CONCLUSIONS

For the first time, a dicopper ion-bound superoxide/peroxide electron-transfer equilibrium has been observed, that for the pair of dicopper(II) complexes $[Cu^{II}_2(UN\text{-}O^-)(O_2^{\bullet-})]^{2+}$ (**2**) and $[Cu^{II}_2(UN\text{-}O^-)(O_2^{2-})]^{+}$ (**3**), providing a superoxide-to-peroxide reduction potential of $E^\circ = +0.13$ V vs SCE, in dichloromethane as solvent. The binucleating ligand UN-O^- facilitated such chemistry, stabilizing both superoxide and peroxide entities (Figure 7). These synthetic complexes or

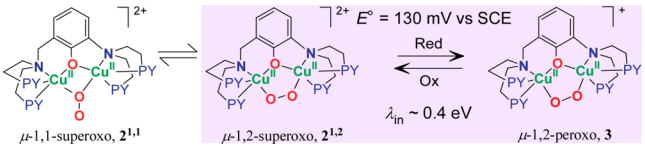

Figure 7. Interconversion of the μ-1,2-peroxide **3**, and the μ-1,2-superoxide $\mathbf{2}^{1,2}$, and equilibrium of μ-1,2-superoxide and μ-1,1-superoxide complexes.

related ones have the potential to serve as models for certain O_2-activating copper proteins with known or putative dicopper active sites. These include tyrosinase,[55] *particulate*-methane monooxygenase (pMMO)[55,56] and possibly even human dopamine β-hydroxylase.[57] As discussed, the one-electron reduction potential for the superoxo/peroxo (**2**/**3**) redox pair found here falls into the biologically relevant region when comparing this value with the existing literature (Table 2), even though solvent and other conditions are different.

The small inner sphere reorganization energy λ_{in} of the peroxo complex **3** oxidation to the superoxo complex $\mathbf{2}^{1,2}$, calculated to be 0.4 eV, suggests the interconversion of $\mathbf{2}^{1,2}$ and **3** to be highly favorable pathway during electron transfer (Figure 7). The superoxo $\mathbf{2}^{1,2}$ and $\mathbf{2}^{1,1}$ forms are considered to be in fast equilibrium based on mixed-isotope rRaman analysis and DFT calculations.

The total reorganization energy for the cross reaction, as an oxidation, $\mathbf{3} + Me_2Fc^+ \rightarrow \mathbf{2}^{1,2} + Me_2Fc$, is determined to be 1.1 ± 0.2 eV with a small driving force $\Delta G^\circ \sim -0.1$ eV. This low λ value and a small thermodynamic driving force make this system quite interesting compared to more complex redox enzymes that typically have electron transfer reorganization energy $\lambda \leq 1.0$ eV and rather small thermodynamic driving forces, $\Delta G^\circ \leq -0.3$ eV.[53]

The thermodynamics of metal-bound superoxo−peroxo interconversion reactions are important to determine for fundamental reasons. How with ligand design can we use coordination chemistry to control reduction potentials and subsequent reactivity? Do reduction potentials even correlate to reactivity, or the type of chemistry involved, e.g., H atom abstraction, proton-coupled electron transfer (PCET) or atom transfer (oxo-transfer)?[58] Does the metal-superoxide to metal-

DOI: 10.1021/jacs.6b02404
J. Am. Chem. Soc. 2016, 138, 7055−7066

peroxide (without or with a proton) reduction potential relate or correlate to the facility toward subsequent reductive O−O bond cleavage, as required and occurring in biological oxidases or fuel-cells? Is a metal ion bound peroxide moiety a necessary intermediate to pass on to an O−O reductive cleavage step? If it is, to what metalation and/or protonation state of the O_2^{2-} fragment required.

The fundamental thermodynamics and electron-transfer properties of these dicopper(II) peroxo and superoxo complexes, with E° = +130 mV vs SCE and a reorganization energy of 1.1 eV makes this system biologically relevant in the sense that these compounds or others may be useful in understanding redox processes in more complex biological systems. Expansion of such investigations, for example to situations with a single copper ion (and not in a binuclear complex) is certainly required for us to fully understand important reactions involving O_2 and its reduced derivatives, which critically apply to our societal energy outlook.

EXPERIMENTAL SECTION

Refer to Supporting Information for experimental details and related instrumentation.

ASSOCIATED CONTENT

Supporting Information

The Supporting Information is available free of charge on the ACS Publications website at DOI: 10.1021/jacs.6b02404.

Experimental details and data pertaining to X-ray crystallography, various spectroscopies (UV−vis, resonance Raman, NMR, EPR), cyclic voltammetry and redox titrations, kinetics/thermodynamics and Density Functional Theory (DFT) calculations. (PDF)

Crystal data CIF-002 (CIF)

Crystal data CIF-003 (CIF)

Crystal data CIF-004 (CIF)

AUTHOR INFORMATION

Corresponding Authors

*edward.solomon@stanford.edu

*fukuzumi@chem.eng.osaka-u.ac.jp

*karlin@jhu.edu

Present Addresses

[⊥]Department of Chemistry, University of Utah, 315 S 1400 E, Salt Lake City, Utah 84112−0850, United States.

[‖]ZS Associates, Inc., 400 South El Camino Real, Suite 1500, San Mateo, California 94402, United States.

Notes

The authors declare no competing financial interest.

ACKNOWLEDGMENTS

This work was supported by the National Institutes of Health (NIH) (DK031450 to E.I.S.; GM28962 to K.D.K.). M.K.E. was supported by an NIH postdoctoral fellowship (GM085914). C.S. is grateful for research support from the National Research Foundation of Korea, Grant NRF-2015H1D3A1066507. Computational resources were provided in part by the Extreme Science and Engineering Discovery Environment (XSEDE), which is supported by National Science Foundation grant number ACI-1053575 (TG-CHE130047 to M.K.E.) and JSPS (16H02268 to S.F.) from MEXT, Japan.

REFERENCES

(1) (a) Babcock, G. T.; Wikström, M. *Nature* **1992**, *356*, 301. (b) Yoshikawa, S.; Shimada, A. *Chem. Rev.* **2015**, *115*, 1936.

(2) Field, C. B.; Behrenfeld, M. J.; Randerson, J. T.; Falkowski, P. *Science* **1998**, *281*, 237.

(3) However, for a case in cobalt cluster chemistry, see: Zhang, M.; de Respinis, M.; Frei, H. *Nat. Chem.* **2014**, *6*, 362.

(4) Koppenol, W. H.; Stanbury, D. M.; Bounds, P. L. *Free Radical Biol. Med.* **2010**, *49*, 317.

(5) (a) Meunier, B.; de Visser, S. P.; Shaik, S. *Chem. Rev.* **2004**, *104*, 3947. (b) Shaik, S.; Cohen, S.; Wang, Y.; Chen, H.; Kumar, D.; Thiel, W. *Chem. Rev.* **2010**, *110*, 949.

(6) (a) Mirica, L. M.; Ottenwaelder, X.; Stack, T. D. P. *Chem. Rev.* **2004**, *104*, 1013. (b) Itoh, S. *Curr. Opin. Chem. Biol.* **2006**, *10*, 115. (c) Hatcher, L. Q.; Karlin, K. D. *JBIC, J. Biol. Inorg. Chem.* **2004**, *9*, 669. (d) Gagnon, N.; Tolman, W. B. *Acc. Chem. Res.* **2015**, *48*, 2126.

(7) Lee, J. Y.; Karlin, K. D. *Curr. Opin. Chem. Biol.* **2015**, *25*, 184.

(8) Mahroof-Tahir, M.; Karlin, K. D. *J. Am. Chem. Soc.* **1992**, *114*, 7599.

(9) (a) Mahroof-Tahir, M.; Murthy, N. N.; Karlin, K. D.; Blackburn, N. J.; Shaikh, S. N.; Zubieta, J. *Inorg. Chem.* **1992**, *31*, 3001. (b) If Ag^+ ion is added to peroxo-dicopper(II) complex **3**, it converts to superoxo-dicopper(II) complex **2**.

(10) Thorp, H. H. *Inorg. Chem.* **1992**, *31*, 1585.

(11) Addison, A. W.; Rao, T. N.; Reedijk, J.; van Rijn, J.; Verschoor, G. C. *J. Chem. Soc., Dalton Trans.* **1984**, 1349.

(12) Robin, M. B.; Day, P. *Adv. Inorg. Chem. Radiochem.* **1968**, *10*, 247.

(13) Cruse, R. W.; Kaderli, S.; Karlin, K. D.; Zuberbühler, A. D. *J. Am. Chem. Soc.* **1988**, *110*, 6882.

(14) Saracini, C.; Liakos, D. G.; Rivera, J. E. Z.; Neese, F.; Meyer, G. J.; Karlin, K. D. *J. Am. Chem. Soc.* **2014**, *136*, 1260.

(15) Weitzer, M.; Schindler, S.; Brehm, G.; Schneider, S.; Hoermann, E.; Jung, B.; Kaderli, S.; Zuberbuehler, A. D. *Inorg. Chem.* **2003**, *42*, 1800.

(16) Kunishita, A.; Ertem, M. Z.; Okubo, Y.; Tano, T.; Sugimoto, H.; Ohkubo, K.; Fujieda, N.; Fukuzumi, S.; Cramer, C. J.; Itoh, S. *Inorg. Chem.* **2012**, *51*, 9465.

(17) Aboelella, N. W.; Kryatov, S. V.; Gherman, B. F.; Brennessel, W. W.; Young, V. G.; Sarangi, R.; Rybak-Akimova, E. V.; Hodgson, K. O.; Hedman, B.; Solomon, E. I.; Cramer, C. J.; Tolman, W. B. *J. Am. Chem. Soc.* **2004**, *126*, 16896.

(18) Fry, H. C.; Scaltrito, D. V.; Karlin, K. D.; Meyer, G. J. *J. Am. Chem. Soc.* **2003**, *125*, 11866.

(19) Kobayashi, Y.; Ohkubo, K.; Nomura, T.; Kubo, M.; Fujieda, N.; Sugimoto, H.; Fukuzumi, S.; Goto, K.; Ogura, T.; Itoh, S. *Eur. J. Inorg. Chem.* **2012**, *2012*, 4574.

(20) Maiti, D.; Fry, H. C.; Woertink, J. S.; Vance, M. A.; Solomon, E. I.; Karlin, K. D. *J. Am. Chem. Soc.* **2007**, *129*, 264.

(21) The mixed isotope experiments conclusively demonstrate that the origin of these features are from a μ-1,1-adduct because of lack of observation of a peak "in the middle" of the ^{16}O−Cu and ^{18}O−Cu features, which would result from a μ-1,2 adduct at the average of the two stretches. Within the quality of our data, we are unable to locate a Cu−O stretch from the μ-1,2 component, which suggests that it must have either or both a weak intensity and/or is underneath the isotope sensitive bands we are observing. The increased intensity of the O−O could be linked to a decreased intensity of the Cu−O. However, this level of analysis is not possible given (1) the quality of the data as these are all weak features, and (2) the complications from all the different ligand conformational isomers. Five batches of samples were used, and the experimental results were in agreement. Thus, we choose to not speculate on this point in the manuscript, as the O−O region is diagnostic regarding the presence of μ-1,1 and μ-1,2 superoxides.

(22) Noviandri, I.; Brown, K. N.; Fleming, D. S.; Gulyas, P. T.; Lay, P. A.; Masters, A. F.; Phillips, L. *J. Phys. Chem. B* **1999**, *103*, 6713.

(23) The DFT calculations suggest there may be seven μ-1,2-peroxide conformers with small ligand conformation changes and energies different from 0.7 to 2.9 kcal/mol (determined at −80 °C) compared to the one with lowest energy, Figure S10−S12. There are also three μ-1,1-superoxide and seven μ-1,2-superoxide species, which differ by only small ligand conformation changes and which possess energy differences

DOI: 10.1021/jacs.6b02404
J. Am. Chem. Soc. 2016, 138, 7055−7066

of between 1.7 to 4.8 kcal/mol (Figure S3−S6). Therefore, we consider the energy differences between the μ-1,1-superoxide and μ-1,2-superoxide isomers are on the same order of magnitude for different ligand conformation changes and thus has very small if any influence on the overall superoxide/peroxide equilibrium constant or the reduction potential.

(24) (a) Vad, M. S.; Nielsen, A.; Lennartson, A.; Bond, A. D.; McGrady, J. E.; McKenzie, C. J. *J. Chem. Soc., Dalton Trans.* **2011**, *40*, 10698. (b) Vad, M. S.; Johansson, F. B.; Seidler-Egdal, R. K.; McGrady, J. E.; Novikov, S. M.; Bozhevolnyi, S. I.; Andrew, D.; Bond, A. D.; McKenzie, C. J. *J. Chem. Soc., Dalton Trans.* **2013**, *42*, 9921.

(25) If Ag^+ ion is added to peroxo-dicopper(II) complex **3**, it converts to superoxo-dicopper(II) complex **2**.

(26) (a) Especially for CH_2Cl_2 vs ACN vs acetone as solvents, the E° values determined (often by cyclic voltammetry; $E_{1/2}$) are very close, within ∼20 mV, as long as a similar electrolyte is employed in the experiments. Depending on the type of compounds used, E° in DMF can vary by as much as a few hundred mV from these other solvents. (b) Barriere, F.; Camire, N.; Geiger, W. E.; Mueller-Westerhoff, U. T.; Sanders, R. *J. Am. Chem. Soc.* **2002**, *124*, 7262. (c) Barriere, F.; Geiger, W. E. *J. Am. Chem. Soc.* **2006**, *128*, 3980. (d) Srivastava, K.; Srivastava, A. K.; Porwal, D.; Prasad, J. *J. Indian Chem. Soc.* **2007**, *84*, 1195. (e) Sasaki, K.; Kashimura, T.; Ohura, M.; Ohsaki, Y.; Ohta, N. *J. Electrochem. Soc.* **1990**, *137*, 2437. (f) Guirado, G.; Fleming, C. N.; Lingenfelter, T. G.; Williams, M. L.; Zuilhof, H.; Dinnocenzo, J. P. *J. Am. Chem. Soc.* **2004**, *126*, 14086. (g) Svith, H.; Jensen, H.; Almstedt, J.; Andersson, P.; Lundback, T.; Daasbjerg, K.; Jonsson, M. *J. Phys. Chem. A* **2004**, *108*, 4805. (h) Konezny, S. J.; Doherty, M. D.; Luca, O. R.; Crabtree, R. H.; Soloveichik, G. L.; Batista, V. S. *J. Phys. Chem. C* **2012**, *116*, 6349. (i) Araujo, C. M.; Doherty, M. D.; Konezny, S. J.; Luca, O. R.; Usyatinsky, A.; Grade, H.; Lobkovsky, E.; Soloveichik, G. L.; Crabtree, R. H.; Batista, V. S. *J. Chem. Soc., Dalton Trans.* **2012**, *41*, 3562.

(27) (a) McLendon, G.; Mooney, W. F. *Inorg. Chem.* **1980**, *19*, 12. (b) Richens, D. T.; Sykes, A. G. *J. Chem. Soc., Dalton Trans.* **1982**, 1621.

(28) Henthorn, J. T.; Agapie, T. *Angew. Chem., Int. Ed.* **2014**, *53*, 12893.

(29) O'Reilly, N. J.; Magner, E. *Langmuir* **2005**, *21*, 1009.

(30) Warren, J. J.; Mayer, J. M. *J. Am. Chem. Soc.* **2008**, *130*, 7546.

(31) Mase, K.; Ohkubo, K.; Xue, Z. L.; Yamada, H.; Fukuzumi, S. *Chem. Sci.* **2015**, *6*, 6496.

(32) Peterson, R. L.; Ginsbach, J. W.; Cowley, R. E.; Qayyum, M. F.; Himes, R. A.; Siegler, M. A.; Moore, C. D.; Hedman, B.; Hodgson, K. O.; Fukuzumi, S.; Solomon, E. I.; Karlin, K. D. *J. Am. Chem. Soc.* **2013**, *135*, 16454.

(33) Lopez, N.; Graham, D. J.; McGuire, R.; Alliger, G. E.; Shao-Horn, Y.; Cummins, C. C.; Nocera, D. G. *Science* **2012**, *335*, 450.

(34) Chikushi, N.; Nishikami, Y.; Nishide, H. *Chem. Lett.* **2014**, *43*, 760.

(35) Koppenol, W. H. *J. Am. Chem. Soc.* **2007**, *129*, 9686.

(36) Root, D. E.; Mahroof-Tahir, M.; Karlin, K. D.; Solomon, E. I. *Inorg. Chem.* **1998**, *37*, 4838.

(37) (a) Marcus, R. A. *Annu. Rev. Phys. Chem.* **1964**, *15*, 155. (b) Marcus, R. A. *Angew. Chem., Int. Ed. Engl.* **1993**, *32*, 1111.

(38) Marcus, R. A.; Sutin, N. *Biochim. Biophys. Acta, Rev. Bioenerg.* **1985**, *811*, 265.

(39) Nielson, R. M.; Mcmanis, G. E.; Safford, L. K.; Weaver, M. J. *J. Phys. Chem.* **1989**, *93*, 2152.

(40) Saha, S. K.; Ghosh, M. C.; Gould, E. S. *Inorg. Chem.* **1992**, *31*, 5439.

(41) Endicott, J. F.; Kumar, K. Reactivity of Coordinated Dioxygen. In *Mechanistic Aspects of Inorganic Reactions*; American Chemical Society: 1982; Vol. *198*, p 425.

(42) (a) Ghosh, S. P.; Ghosh, M. C.; Gould, E. S. *Int. J. Chem. Kinet.* **1994**, *26*, 665. (b) Ghosh, S. P.; Gelerinter, E.; Pyrka, G.; Gould, E. S. *Inorg. Chem.* **1993**, *32*, 4780.

(43) Anderson, B. L.; Maher, A. G.; Nava, M.; Lopez, N.; Cummins, C. C.; Nocera, D. G. *J. Phys. Chem. B* **2015**, *119*, 7422.

(44) Tahsini, L.; Kotani, H.; Lee, Y.-M.; Cho, J.; Nam, W.; Karlin, K. D.; Fukuzumi, S. *Chem. - Eur. J.* **2012**, *18*, 1084.

(45) (a) Karlin, K. D.; Haka, M. S.; Cruse, R. W.; Meyer, G. J.; Farooq, A.; Gultneh, Y.; Hayes, J. C.; Zubieta, J. *J. Am. Chem. Soc.* **1988**, *110*, 1196. (b) Thyagarajan, S.; Murthy, N. N.; Narducci Sarjeant, A. A.; Karlin, K. D.; Rokita, S. E. *J. Am. Chem. Soc.* **2006**, *128*, 7003.

(46) (a) Karlin, K. D.; Gultneh, Y.; Hayes, J. C.; Cruse, R. W.; McKown, J. W.; Hutchinson, J. P.; Zubieta, J. *J. Am. Chem. Soc.* **1984**, *106*, 2121. (b) Karlin, K. D.; Tyeklár, Z.; Farooq, A.; Haka, M. S.; Ghosh, P.; Cruse, R. W.; Gultneh, Y.; Hayes, J. C.; Toscano, P. J.; Zubieta, J. *Inorg. Chem.* **1992**, *31*, 1436.

(47) (a) Fukuzumi, S.; Kotani, H.; Lucas, H. R.; Doi, K.; Suenobu, T.; Peterson, R. L.; Karlin, K. D. *J. Am. Chem. Soc.* **2010**, *132*, 6874. (b) Fukuzumi, S.; Karlin, K. D. *Coord. Chem. Rev.* **2013**, *257*, 187.

(48) (a) Lee, Y.-M.; Kotani, H.; Suenobu, T.; Nam, W.; Fukuzumi, S. *J. Am. Chem. Soc.* **2008**, *130*, 434. (b) Fukuzumi, S. *Coord. Chem. Rev.* **2013**, *257*, 1564.

(49) Skov, L. K.; Pascher, T.; Winkler, J. R.; Gray, H. B. *J. Am. Chem. Soc.* **1998**, *120*, 1102.

(50) Fukuzumi, S.; Kotani, H.; Prokop, K. A.; Goldberg, D. P. *J. Am. Chem. Soc.* **2011**, *133*, 1859.

(51) Lind, J.; Shen, X.; Merenyi, G.; Jonsson, B. O. *J. Am. Chem. Soc.* **1989**, *111*, 7654.

(52) Roth, J. P.; Klinman, J. P. *Proc. Natl. Acad. Sci. U. S. A.* **2003**, *100*, 62.

(53) (a) Heller, A. *Acc. Chem. Res.* **1990**, *23*, 128. (b) Gray, H. B.; Winkler, J. R. *Annu. Rev. Biochem.* **1996**, *65*, 537. (c) Warshel, A.; Sharma, P. K.; Kato, M.; Xiang, Y.; Liu, H. B.; Olsson, M. H. M. *Chem. Rev.* **2006**, *106*, 3210.

(54) Solomon, E. I.; Szilagyi, R. K.; George, S. D.; Basumallick, L. *Chem. Rev.* **2004**, *104*, 419.

(55) Solomon, E. I.; Heppner, D. E.; Johnston, E. M.; Ginsbach, J. W.; Cirera, J.; Qayyum, M.; Kieber-Emmons, M. T.; Kjaergaard, C. H.; Hadt, R. G.; Tian, L. *Chem. Rev.* **2014**, *114*, 3659.

(56) Citek, C.; Lin, B.-L.; Phelps, T. E.; Wasinger, E. C.; Stack, T. D. P. *J. Am. Chem. Soc.* **2014**, *136*, 14405.

(57) Vendelboe, T. V.; Harris, P.; Zhao, Y.; Walter, T. S.; Harlos, K.; El Omari, K.; Christensen, H. E. M. *Sci. Adv.* **2016**, *2*, e1500980.

(58) Ray, K.; Pfaff, F. F.; Wang, B.; Nam, W. *J. Am. Chem. Soc.* **2014**, *136*, 13942.

NOTE ADDED IN PROOF

With respect to the determination of the (**2**)/(**3**) reduction potential, we repeated several of the experiments involving ferrocenium derivative oxidation of peroxodicopper(II) complex **3** but now in the presence of 0.1 M nBu_4NPF_6; the results were unchanged compared to those carried out in the absence of this electrolyte.

DOI: 10.1021/jacs.6b02404
J. Am. Chem. Soc. 2016, 138, 7055−7066